

Study of L-subshell ionization by proton Bombardment
of Pb and Bi

H.C. Padhi, C.R. Bhuinya, B.B. Dhal and S. Misra

Institute of Physics, Bhubaneswar-751005, India.

Abstract:

L X-ray production cross-sections and relative intensities of Pb and Bi have been measured for proton ionization in the energy range 1 to 4 MeV. The measured cross-sections are in good agreement with the theoretical results obtained from ECPSSR ionization cross-sections of Cohen and Harrigan (1985) and different decay yield (Krause 1979, Xu and Xu 1992) data. The experimental X-ray production cross-sections for Bi, however, are found to be somewhat higher compared to the theoretical results obtained from RPWBA-DHS-BC ionization cross-sections of Chen and Crasemann (1989) and decay yields of Chen et al (1981). Unlike the earlier results of Xu and Xu (1992) our present results on relative L_i X-ray yields suggest that from the presently available decay yield data sets no one is giving complete agreement with the experimental data. The centroid energies of L_α and L_β peaks of both Pb and Bi remain same with proton energy while the L_γ centroid energy changes by about 50 eV. The experimental centroid energies are in good agreement with ECPSSR and RPWBA-DHS-BC theoretical predictions.



IP - BBSR - 93 - 13
- IP - BBSR - 93 - B

In recent times measurement of inner-shell ionization cross-sections by charged particle bombardment has been of great interest for checking the results of various model calculations. Although a great amount of understanding has been achieved in explaining the experimental data on K-shell ionization cross-sections the situation is not so clear in the case of L-shell ionization. This has been evident from some existing comparison works of Gray 1990 and Cohen (1990). Another problem with L-subshell ionization has been lack of proper fluorescence and Coster-Kronig decay yield data for conversion of the measured X-ray production cross-sections into L_i subshell ionization cross-sections. Moreover there are several approaches for determining ionization cross-sections from measured x-ray yields (Cohen 1984) leading to different results and it is difficult to decide which approach is more reliable. Consequently, a detailed comparison of existing subshell ionization data with various theoretical descriptions becomes difficult. Also presently available data on L_i X-ray production cross-sections for elements in different regions of the periodic table for proton bombardment is sparse and more measurements are needed for a systematic check on the results of various model calculations of atomic ionization. Recently X-ray production cross-sections in Pb and Bi have theoretically been calculated by Xu and Xu (1992) using ECPSSR (Cohen and Harrigan 1985) and RPWBA-DHS-BC (Chen and Crasemann 1989) ionization cross-sections and different sets of fluorescence and Coster-Kronig decay yield data (Krause 1979, Xu and Xu 1992, Chen 1981, Werner and Jitschen 1989) and it was shown by them that the theoretical results obtained from ECPSSR ionization cross-section and fluorescence yield data of Xu and Xu fits well with the experimental data on relative X-ray production cross-sections of Pb and Bi whereas the Krause's decay yield data underestimates the L_i X-ray relative intensities.

The purpose of the present study is to measure the L_i X-ray yields in Pb and Bi and determine both L_i X-ray relative intensities as well as absolute production cross-sections and compare them with the results of various theoretical calculations using different sets of decay yield data. Another important aspect of the present study is instead of deducing the experimental ionization cross-sections from the measured X-ray yields for comparing with the theory, the X-ray production cross-sections will be directly compared. In doing so we may lose certain informations which are present in the individual L_i -subshell ionization cross-sections but such a comparison will be more reliable.

2. Experimental procedure

High pure (99.9%) samples were used for the preparation of the targets. Thin ($40\mu\text{g}/\text{cm}^2$) targets of Pb and Bi were prepared by vacuum evaporation onto aluminized Mylar films of thickness $1.75\text{mg}/\text{cm}^2$. The targets were bombarded by protons with energy 1.07 to 4.07 MeV obtained from the 3MV tandem pelletron accelerator of the Institute. To obtain the L_i X-ray production cross-sections, simultaneous X-ray and elastically scattered charged particle detection technique was employed. A schematic diagram of the experimental chamber is shown in fig.1. The collimated beam of 1.5 mm diameter was directed onto the target which was kept tilted at 45° to the beam direction. The emitted L X-rays passed through a $3.5\text{mg}/\text{cm}^2$ Mylar chamber window, 5 mm air-gap and 0.012 mm thick beryllium window before reaching the Si(Li) detector having an energy resolution of 170 eV (FWHM) at 5.9 KeV. The detector was placed at 90° to the beam direction. A typical X-ray spectrum of bismuth at 1.57 MeV proton energy is shown in fig.2.

3. Data analysis

From the measured X-ray yields the L_i X-ray production cross-sections were esti-

ated using the following relation:

$$\sigma_{L_i}^i = \frac{4\pi Y_r^i \sigma_R(\theta) \Delta\Omega_p}{\epsilon_a \epsilon_d Y_R \Delta\Omega_r} \left(\frac{t_r}{t_d} \right) \dots \quad (1)$$

where

- $\sigma_{L_i}^i$ = X-ray production cross-section (i stands for $d_{1,2}, \beta_{1,3,5}, \gamma_{1,2}$ etc).
- $\sigma_R(\theta)$ = differential Rutherford scattering cross-section
- Y_r^i = Measured X-ray yield for the i^{th} L X-ray peak.
- Y_R = Measured Rutherford yield
- ϵ_d = detector efficiency
- ϵ_a = absorption correction for Mylar window and air path
- $\Delta\Omega_p$ = Solid angle subtended by the charged particle silicon surface barrier detector.
- $\Delta\Omega_r$ = solid angle subtended by the Si(Li) X-ray detector.
- t_r = dead-time correction for X-ray counting
- t_d = dead-time correction for charged particle counting.

Efficiency of the Si(Li) detector was theoretically calculated using the following expression:

$$\epsilon_d(E) = e^{-(\mu_{Be} x_{Be} + \mu_{Au} x_{Au} + \mu_{Si} \Delta x_{Si})} (1 - e^{-\mu_{Si} x_{Si}}) \quad (2)$$

where μ 's are the absorption coefficients due to Be window of the detector, the gold layer on the Si(Li) crystal and Si(Li) crystal at the X-ray energy E. Δx_{Si} is the thickness of the insensitive region of the Si(Li) crystal. The absorption coefficients are taken from the table of Hubbel et al (1974). Y_r^i and Y_R^i are obtained from the measured X-ray and Rutherford back scattered spectra, respectively. The X-ray yields for the various X-ray peaks were estimated by the least-square peak fitting method and the Rutherford backscattered (RBS) yields were calculated by summing the counts under the RBS peak.

Corrections due to absorption in the Mylar window and air-path were applied in the usual manner. Correction due to self-absorption in the sample was found to be negligible.

4. Calculation of X-ray production cross-section

Theoretical L_i X-ray production cross-sections are calculated using ECPSSR L_i -subshell ionization cross-sections of Cohen and Harrigan (1985) in the following relations:

$$\sigma_{L_i}^x = (\sigma_{L_1} f_{13} + \sigma_{L_1} f_{12} f_{23} + \sigma_{L_2} f_{23} + \sigma_{L_3}) \omega_3 F_{3i} \quad (3a)$$

$$\sigma_{L_\alpha}^x = (\sigma_{L_1} f_{13} + \sigma_{L_1} f_{12} f_{23} + \sigma_{L_2} f_{23} + \sigma_{L_3}) \omega_3 F_{3\alpha} \quad (3b)$$

$$\begin{aligned} \sigma_{L_\beta}^x &= \sigma_{L_1} \omega_1 f_{1\beta} + (\sigma_{L_1} f_{12} + \sigma_{L_2}) \omega_2 F_{2\beta} \\ &+ (\sigma_{L_1} f_{13} + \sigma_{L_1} f_{12} f_{23} + \sigma_{L_2} f_{23} + \sigma_{L_3}) \omega_3 F_{3\beta} \end{aligned} \quad (3c)$$

$$\sigma_{L_\gamma}^x = \sigma_{L_1} \omega_1 f_{1\gamma} + (\sigma_{L_1} f_{12} + \sigma_{L_2}) \omega_2 F_{2\gamma} \quad (3d)$$

where $\sigma_{L_i}^x$, $\sigma_{L_\alpha}^x$, $\sigma_{L_\beta}^x$ and $\sigma_{L_\gamma}^x$ are the X-ray production cross-sections of the components L_i , L_α , L_β and L_γ , respectively; σ_{L_1} , σ_{L_2} and σ_{L_3} are ionization cross-sections of the subshells L_1 , L_{11} and L_{111} , respectively; ω_1 , ω_2 and ω_3 are the corresponding subshell fluorescence yields; F_{ny} (F_{3i} , $F_{3\alpha}$, $F_{3\beta}$, ..., ect) are the fraction of the radiation widths of the subshell L_n (L_1 , L_{11} and L_{111}) contained in the y^{th} spectral line i.e.,

$$F_{ny} = F_{ny}/F_n$$

(for example, $F_{3i} = F_{3i}/F_3$) where F_n is the total radiative width of L_n . The parameters f_{12} , f_{23} and f_{13} are the Coster-Kronig transition probabilities for $L_1 \rightarrow L_{11}$, $L_{11} \rightarrow L_{111}$, $L_1 \rightarrow L_{111}$, respectively (the arrow indicates the direction of the electron vacancy transition between subshells).

The L_i X-ray production cross-sections have been calculated using the theoretical ionization cross-sections and available decay yield data. The method of comparing the theoretical ionization cross-sections with the experimental results obtained from the measured X-ray yields and available decay yield data which has been adopted previously by

some authors (for example Chang et al (1975) is not followed in the present work because of the inherent difficulty in this method as mentioned before.

5. Results and discussion

The measured and theoretical X-ray production cross-sections for lead are shown in fig.3. The theoretical estimations were made using the ECPSSR ionization cross-sections of Cohen and Harrigan and two sets of decay yield data ((i) Krause 1979 (ii) Xu and Xu (1992) and Werner and Jitschin (1989). As is seen from fig.3, the experimental cross-sections are close to both the theoretical results. Comparing the two theoretical results we see that they differ maximum (about 10%) for σ_α^x which is because of the difference in the fluorescence yield factor ω_3 in the two cases. Since all the relative intensities are calculated with respect to σ_α^x , the theoretical relative intensities shown in fig.4 are naturally lower for the Krause's decay yield data. The measured relative intensities are found to agree partly with the Xu and Xu's (1992) result for the low projectile energy and partly with the result obtained using Krause's (1979) decay yield data in the high energy ($E_p \geq 3MeV$) region. This suggests that for total agreement with the experimental relative intensities both the decay yield data have to be different for different projectile energy. This means one has to take into account the formation of multivacancy in the ionization process.

Fig.5 shows the experimental and theoretical X-ray production cross-sections of E. The theoretical estimations are made using the ECPSSR ionization cross-sections and two sets of decay yield data as in the case of lead and another using RPWBA-DH-BC ionization cross-sections of Chen and Crasemann (1989) and decay yield data of Chen et al (1981). As is seen from fig.5, the theoretical X-ray production cross-sections obtained by using RPWBA-DHS-BC ionization cross-sections are slightly lower ($\leq 10\%$)

than the experimental results whereas the two results obtained from ECPSSR ionization cross-sections and different decay yield data are within 5% of the experimental cross-sections. Comparison of the relative intensities in fig.6 suggests that all the theoretical results are equally good, the RPWBA-DHS-BC results showing better agreement in the entire energy region whereas the ECPSSR results with Krause's decay yield giving better agreement in the high energy region and the other calculation with Xu and Xu's decay yield data showing better agreement in the low energy region ($E_p \leq 2.5$ MeV). Our result does not fully support the earlier conclusion reached by Xu and Xu (1992) that their decay yield data is better.

The centroid energies of various L X-ray lines are calculated using the following relations (Bissinger et al 1972):

$$\begin{aligned} \bar{E}_{L\beta} = & \{n_1 w_1 F_{1\beta} \bar{E}_{1\beta} + (n_1 f_{12} n_2) w_2 F_{2\beta} \bar{E}_{2\beta} \\ & + [n_1 (f_{13} + f_{12} f_{23}) + n_2 f_{23} + n_3] w_3 F_{3\beta} \bar{E}_{3\beta}\} / I_{L\beta} \end{aligned} \quad (4)$$

where

$$n_1 = \sigma_{L_1} / \sigma_{L_2}$$

$$n_2 = \sigma_{L_2} / \sigma_{L_3}$$

$$n_3 = 1$$

$$\begin{aligned} I_{L\beta} = & n_1 w_1 F_{1\beta} + (n_1 f_{12} + n_2) w_2 f_{2\beta} \\ & + [n_1 (f_{13} + f_{12} f_{23}) + n_2 f_{23} + n_3] w_3 F_{3\beta} \end{aligned} \quad (5)$$

$$\bar{E}_{j\beta} = \frac{\sum_i \Gamma_{j\beta_i} E_{j\beta_i}}{\sum_i \Gamma_{j\beta_i}} \quad (i = 1, 2, 3) \quad (6)$$

$$\bar{E}_{L\gamma} = \{n_1 w_1 F_{1\gamma} \bar{E}_{1\gamma} + (n_1 f_{12} + n_2) w_2 F_{2\gamma} \bar{E}_{2\gamma}\} / I_{L\gamma} \quad (7)$$

where

$$I_{L\gamma} = n_1 w_1 F_{1\gamma} + (n_1 f_{12} + n_2) w_2 F_{2\gamma} \quad (8)$$

and

$$\bar{E}_{j\gamma} = \frac{\sum_i \Gamma_{j\gamma_i} E_{j\gamma_i}}{\sum_i \Gamma_{j\gamma_i}} \quad (9)$$

In eqns.(6) and (9) $\bar{E}_{j\beta}$ and $\bar{E}_{j\gamma}$ are intensity weighted average energy for L_β and L_γ lines, respectively, $\Gamma_{j\beta_i}$, $\Gamma_{j\gamma_i}$ etc are radiative widths taken from Campbell and Wang (1989) and $E_{j\beta_i}$ and $E_{j\gamma_i}$ are the measured energies taken from Bearden (1967). Centroid energies of Pb are calculated using ECPSSR ionization cross-sections of Cohen and Harrigan (1985) and for Bi the calculations are made using ECPSSR and RPWBA-DHS-BC ionization cross-sections. The measured and theoretical centroid energies for Pb and Bi are compared in fig.7 and fig.8, respectively. Both the measured and theoretical centroid energies of various L lines show similar energy dependence. The L_α and L_β lines remain almost constant within $\leq 5eV$, with proton energy whereas the L_γ line first shows an initial fall becomes minimum between proton energy of 1.5 and 2.0 MeV and then increases. The maximum shift observed for the L_γ centroid energy is $\sim 50eV$ for both Pb and Bi. This is consistent with the both ECPSSR and RPWBA-DHS-BC calculations.

In conclusion we would like to say that both the ECPSSR and RPWBA-DHS-BC theories give reasonable descriptions of the data. Comparison of the results obtained from different decay yield data suggests that they are equally good within the experimental uncertainties.

Finally the authors thank the accelerator operating staff for their help and cooperation during the experiment.

References:

1. Bearden J A 1967 Rev. Mod. Phys. 39, 78.
2. Bissinger G A, Baskin A B, Choi B H and Shafrath S M 1972 Phys. Rev. A6 545 and references therein.
3. Campbell J L and Wang J X, 1989 At. Data Nucl. Data Tables 43, 281.
4. Chang C N, Morgan J F and Blatt S L 1975 Phys. Rev. A11 607.
5. Chen M H, Crasemann B and Mark H 1981 Phys. Rev. A24 177, 1982 Phys. Rev. A26 1243.
6. Chen M H and Crasemann B 1989 At. Data Nucl. Data Tables 41 257.
7. Close D A, Barse R C, Malamify J J and Umbarger C J 1973 Phys. Rev. A8 1873.
8. Cohen D D 1984 J. Phys. B17 3913.
9. Cohen D D and Harrigan M 1985 At. Data Nucl. Data Tables 33 255.
10. Cohen D D 1990 Nucl. Instr. Methods B49 .
11. Gray T J and Malhi N 1990 Bull. Am. Phys. Soc. 55 1713 and references therein.
12. Hubbel J H, McMaster W H, Del Grande N K and Hamellett J H. 1974 in Reun. J A and Hamilton J C (ed) International Tables for X-ray Crystallography Vol.4 (Keynoch Press, Birmingham) 47.
13. Krause M O 1979 J. Phys. Chem. Ref. Data 8 307.
14. Xu J Q and Xu J X 1992 J. Phys. B25, 695.
15. Werner U and Jitschin W 1988, Phys. Rev. A38 1009.

Figure Captions

Fig.1 A schematic diagram of the experimental chamber

Fig.2 Typical L X-ray spectra of Pb taken at ^{1.57} MeV proton energy.

Fig.3 (a,b,c,d) L_i X-ray production cross-sections of Pb as a function of proton energy E_p . (cross) present experimental results; —, Computed using ECPSSR cross-sections (Cohen and Harrigan 1985) and L subshell fluorescence yields of Xu and Xu (1992) and Coster-Kronig yields of Werner and Jitschin (1988) - - -, computed by using ECPSSR cross-sections (Cohen and Harrigan 1985) and L-subshell decay yields of Krause (1979).

Fig.4 (a,b,c,d) Intensity ratios of Pb $L_I, L_{\beta}, L_{\gamma}$ and $L_T (L_T = L_I + L_{\alpha} + L_{\beta} - L_{\gamma})$ to L_{α} as a function of proton energy E_p . The experimental points (crosses) joined by a continuous line are from present work; (open circles) computed using ECPSSR ionization cross-sections (Cohen and Harrigan 1985) and fluorescence yields of Xu and Xu (1992) and Coster - Kronig yields of Werner and Jitschin (1988); (open triangle) computed using ECPSSR cross-sections (Cohen and Harrigan 1985) and decay yields of Krause (1979).

Fig.5 (a,b,c,d) L_i X-ray production cross-sections of Bi as a function of proton energy E_p . (crosses) are from present experiment; —, computed using ECPSSR cross-sections (Cohen and Harrigan 1985) and L subshell fluorescence yields of Xu and Xu (1992) and Coster-Kronig yields of Chen et al (1981). - - -, computed by using ECPSSR cross-sections (Cohen and Harrigan 1985) and L-subshell decay yields of Krause (1979);, computed using RPWBA-DHS-BC cross-sections (Chen and Crasemann 1989) and DHS decay yields (Chen et al 1981).

Fig.6 (a,b,c,d) Intensity ratios of Bi $L_I, L_{\beta}, L_{\gamma}$ and $L_T (L_T = L_I + L_{\alpha} + L_{\beta} + L_{\gamma})$ to L_{α} as a function of proton energy E_p . The experimental points (crosses) joined

continuous line are from present work; (open circles) computed using ECPSSR cross-sections (Cohen and Harrigan 1985) and fluorescence yields of Xu and Xu (1992) and Coster-Kronig yields of Chen et al (1981); (open triangles) computed using ECPSSR cross-sections (Cohen and Harrigan 1985) and decay yields of Krause; (solid circles) computed using RPWBA-DHS-BC cross-sections (Chen and Crasemann 1989) and decay yields of Chen et al (1981).

Fig.7 L_{α} , L_{β} , L_{γ} centroid energies plotted as a function of proton energy E_p for Pb: solid lines are eye fitted lines drawn through the experimental points. - - -, computed using ECPSSR ionization cross-sections (Cohen and Harrigan 1985) and decay yields of Krause (1979) and radiative widths of Campbell and Wang (1989).

Fig.8 L_{α} , L_{β} , L_{γ} centroid energies plotted as a function of proton energy E_p for Bi: solid lines are eye fitted lines drawn through the experimental points. - - -, computed using ECPSSR ionization cross-sections (Cohen and Harrigan 1985) and decay yields of Krause (1979);, computed using RPWBA-DHS-BC cross-sections (Chen and Crasemann 1989) and decay yields of Chen et al (1981).

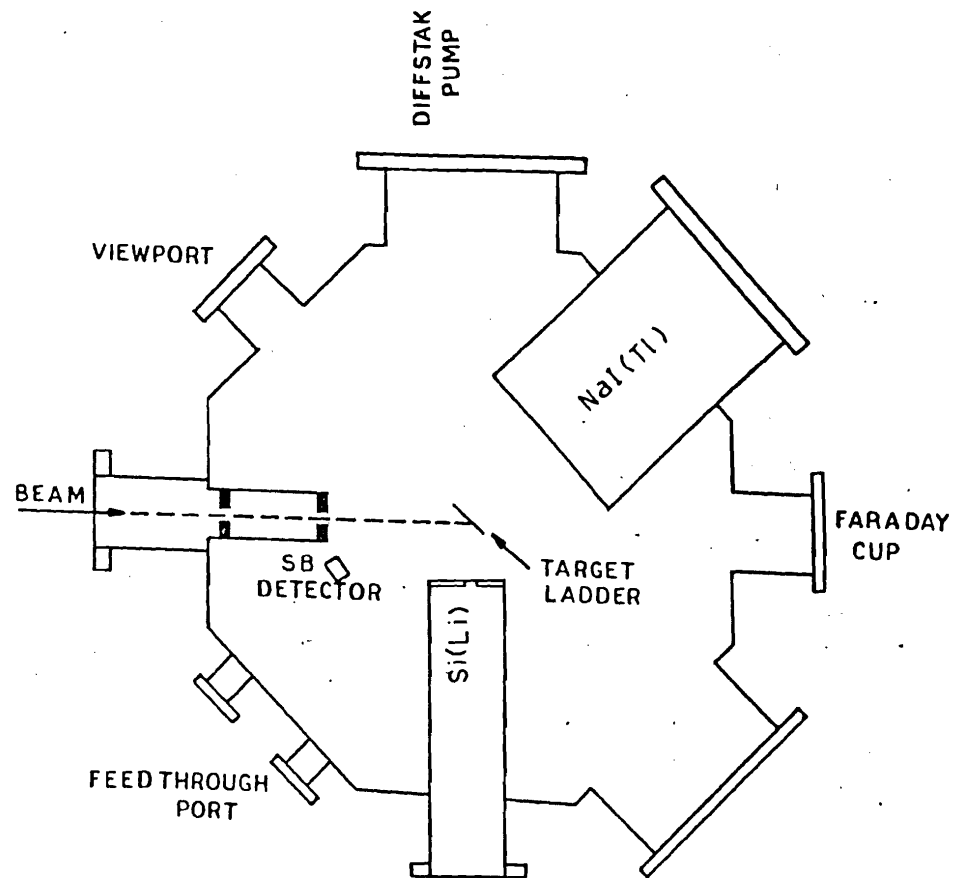
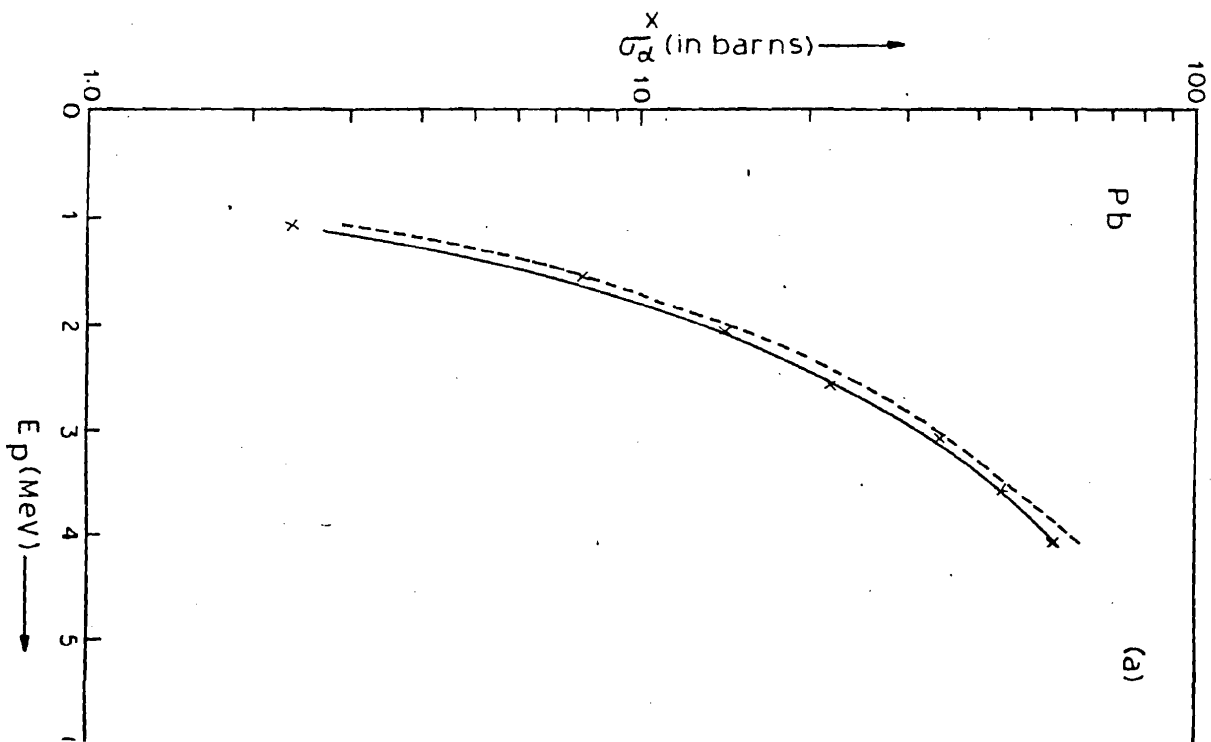
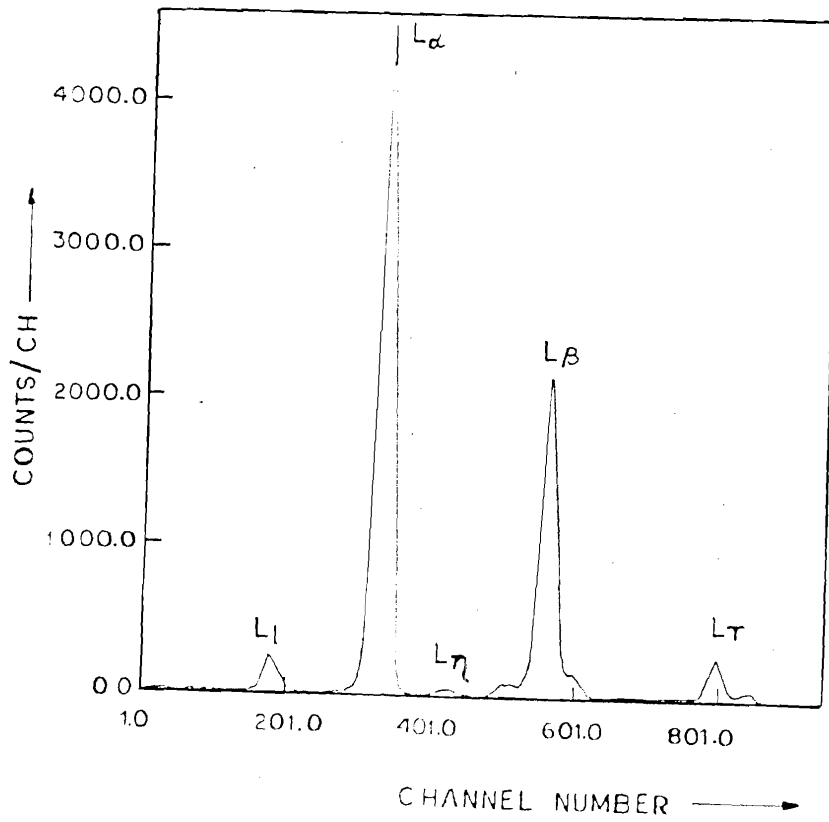
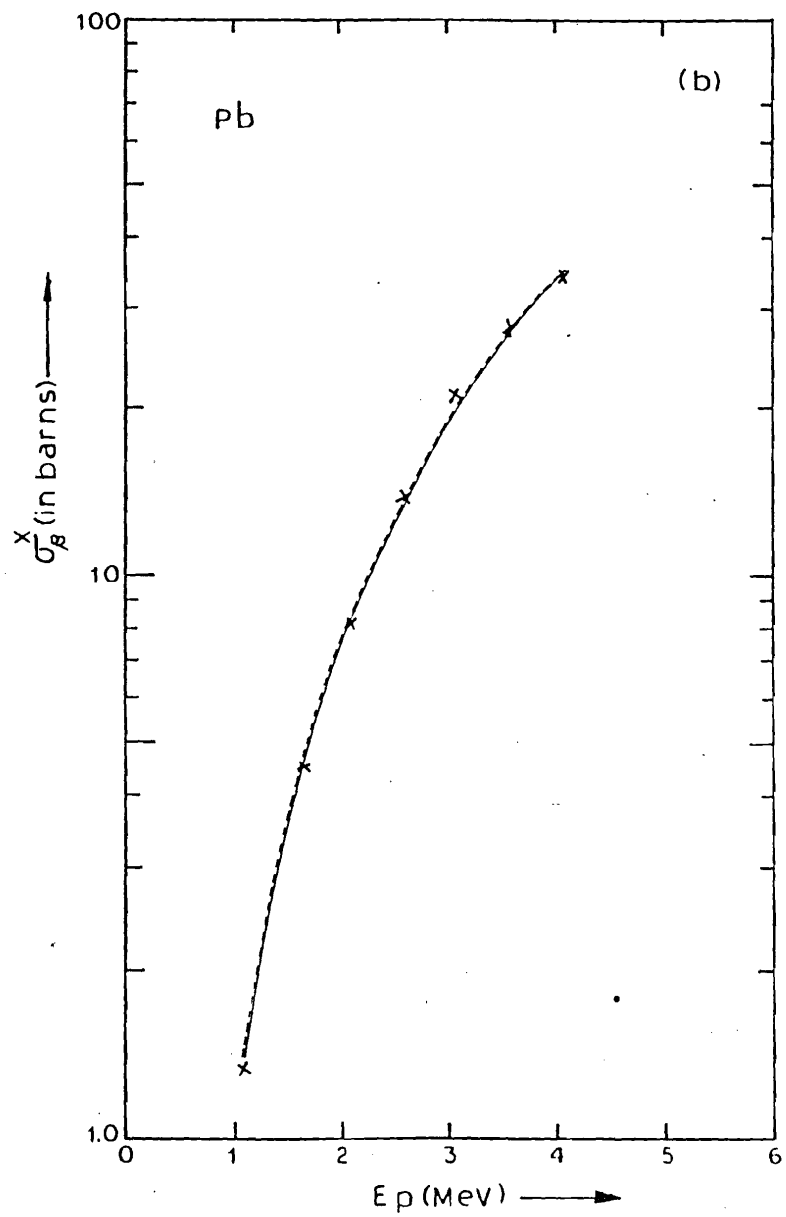
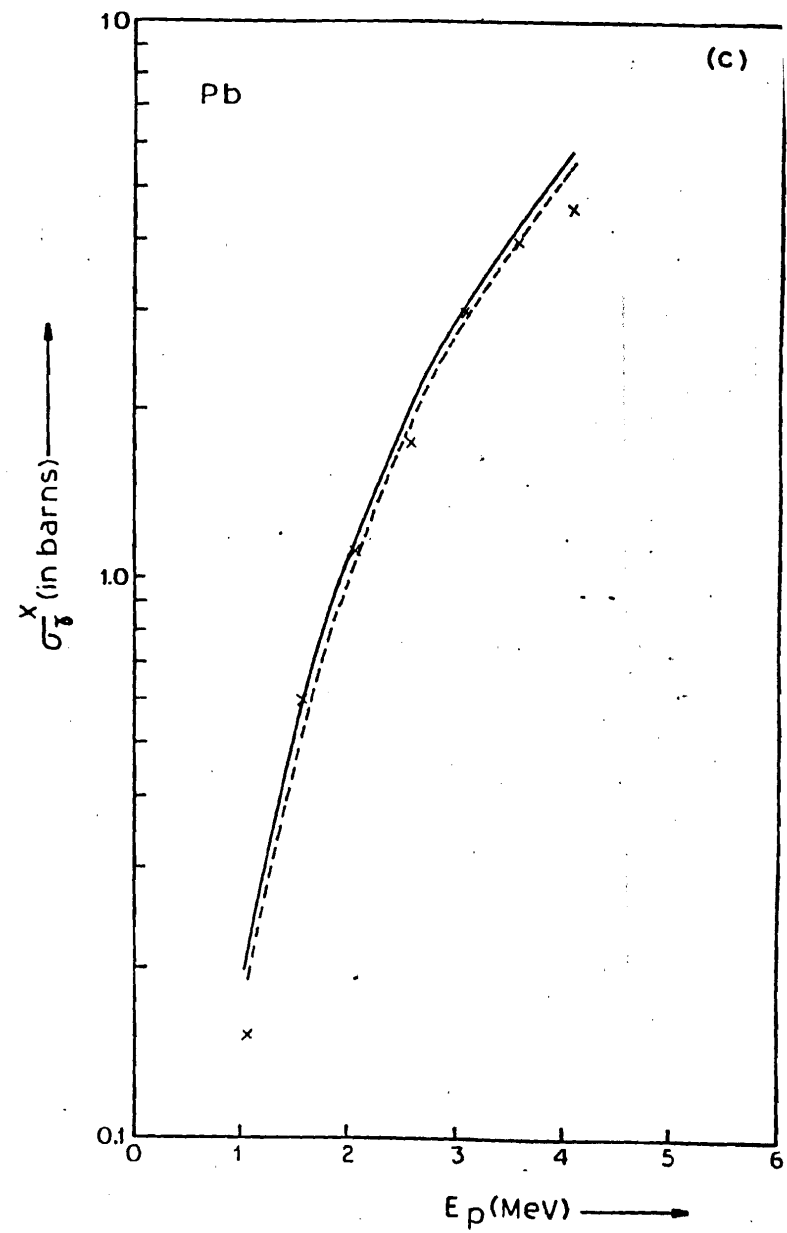


Fig.1

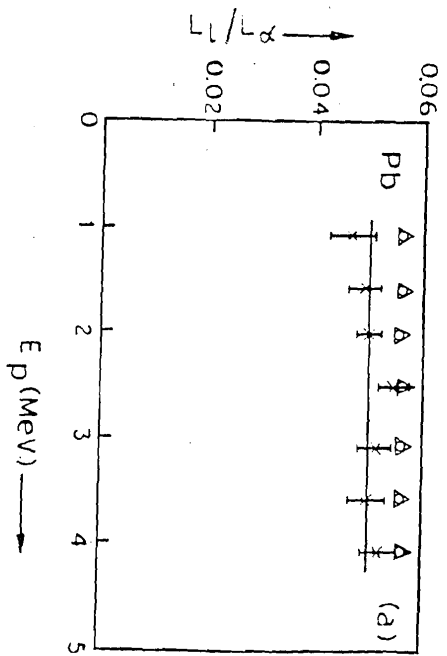
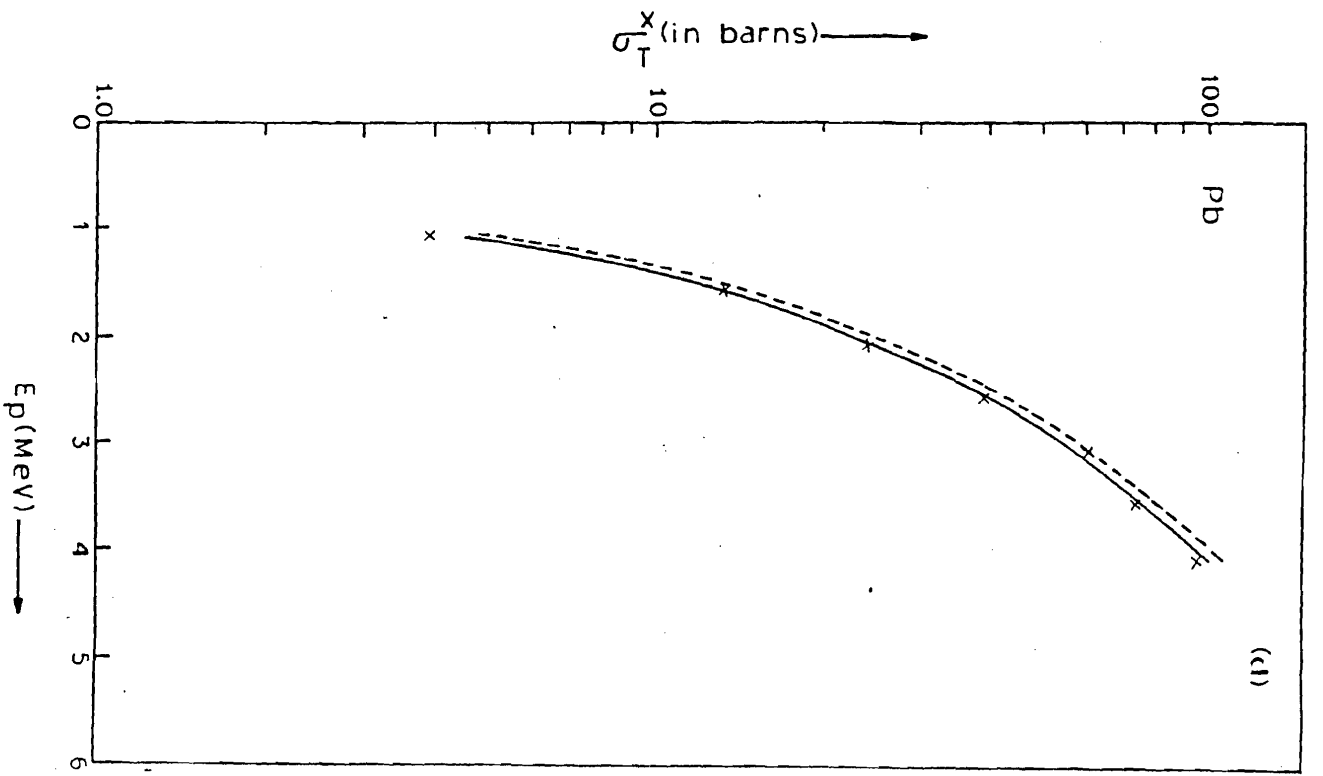


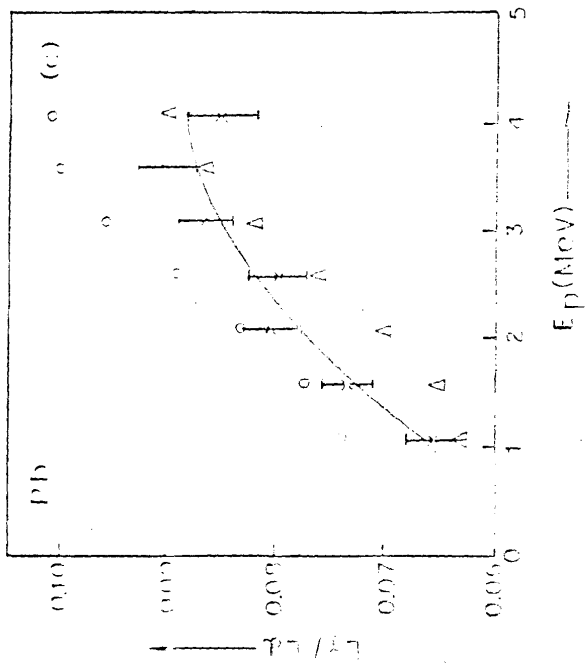
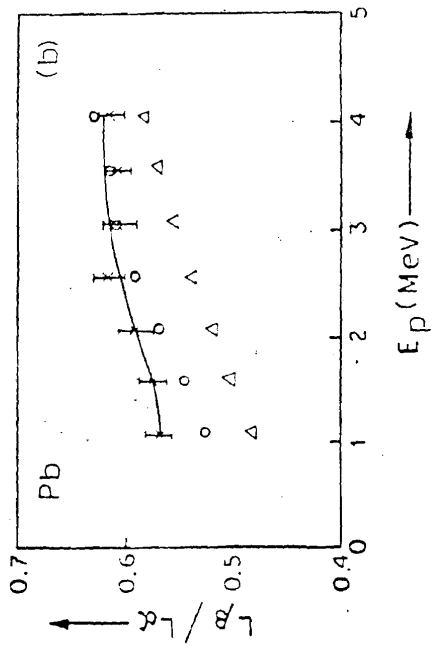


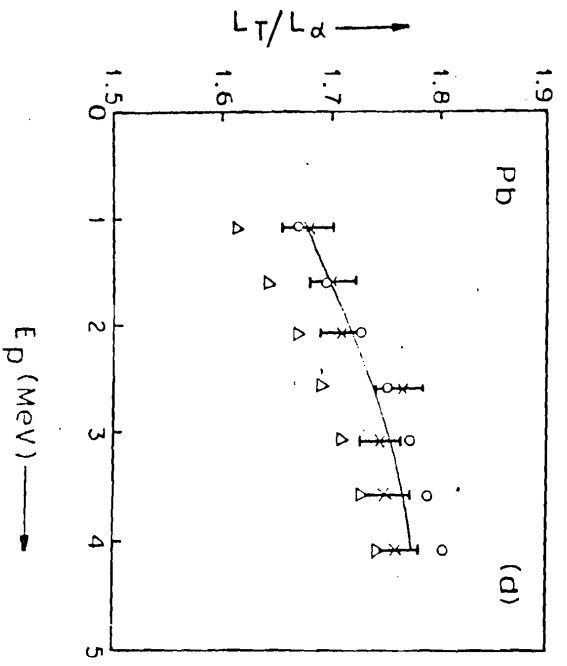
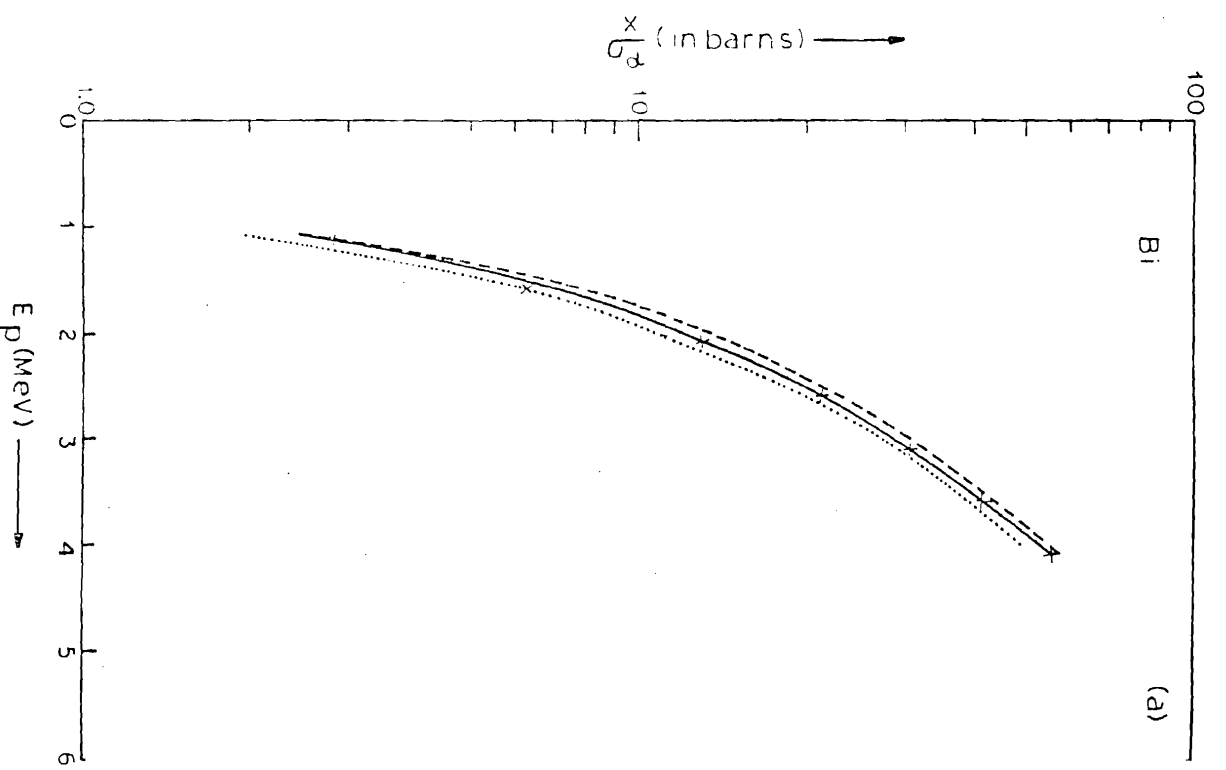
F. 11

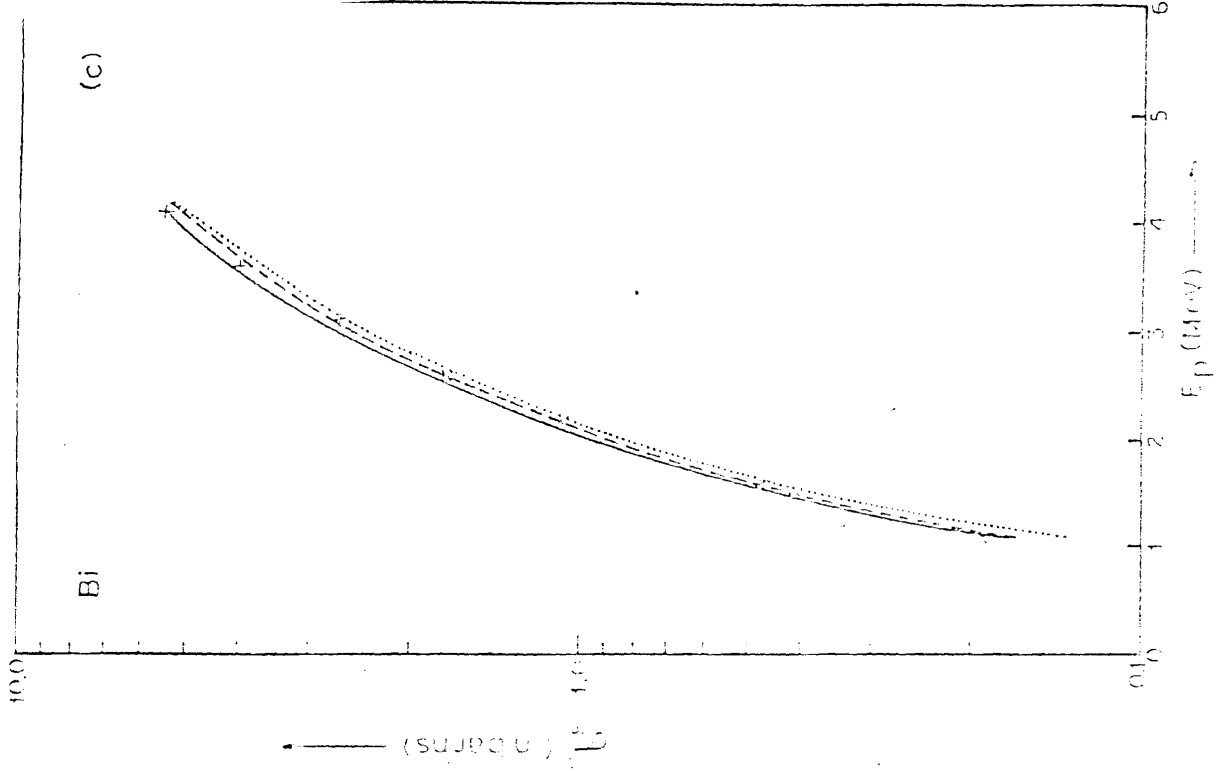
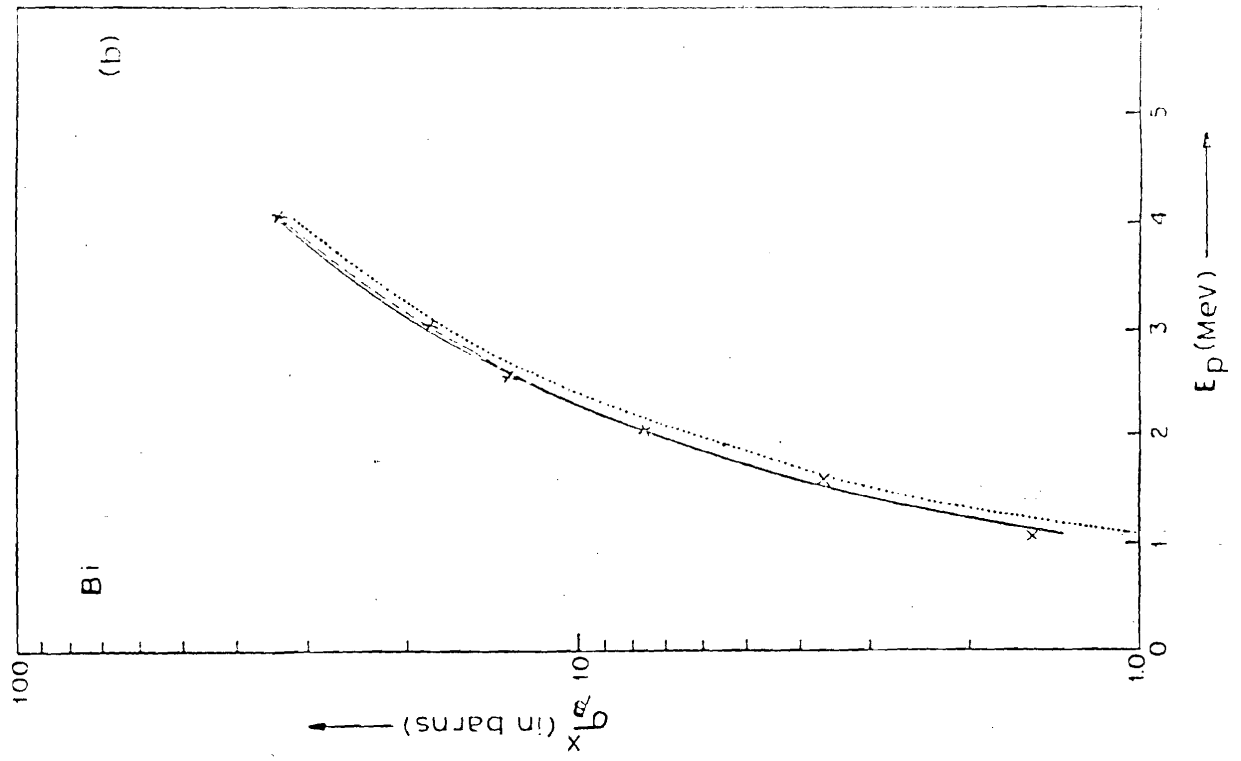


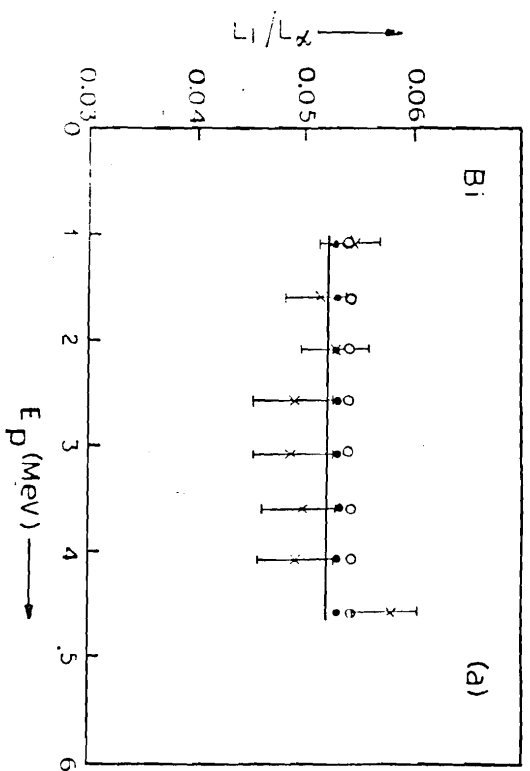
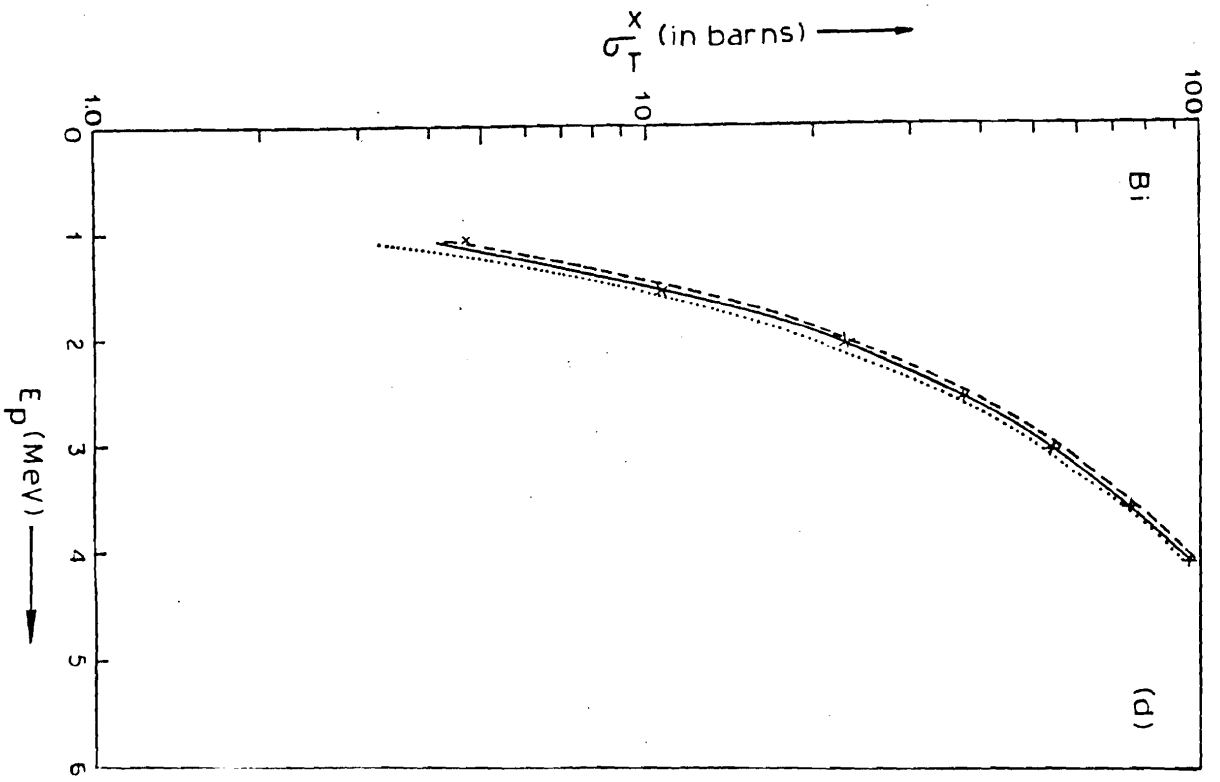
F. 12

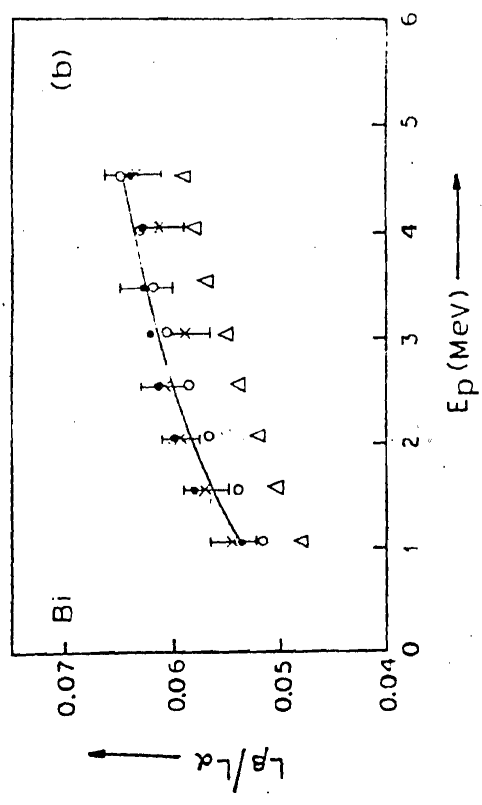
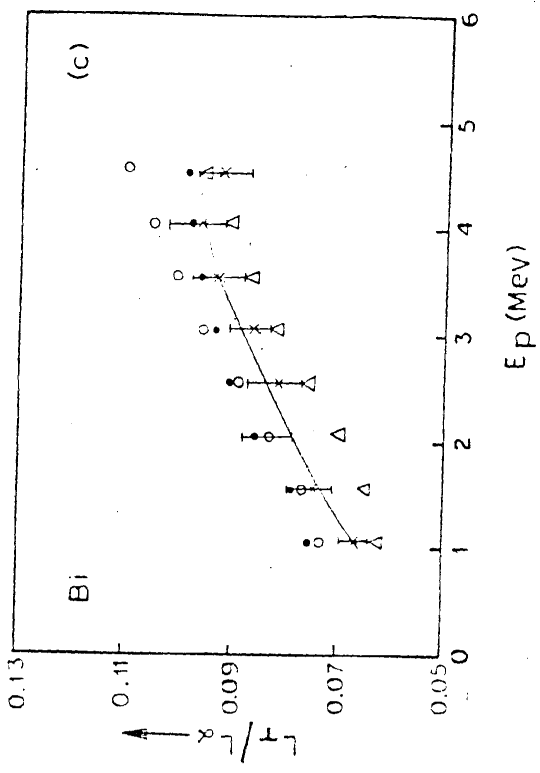












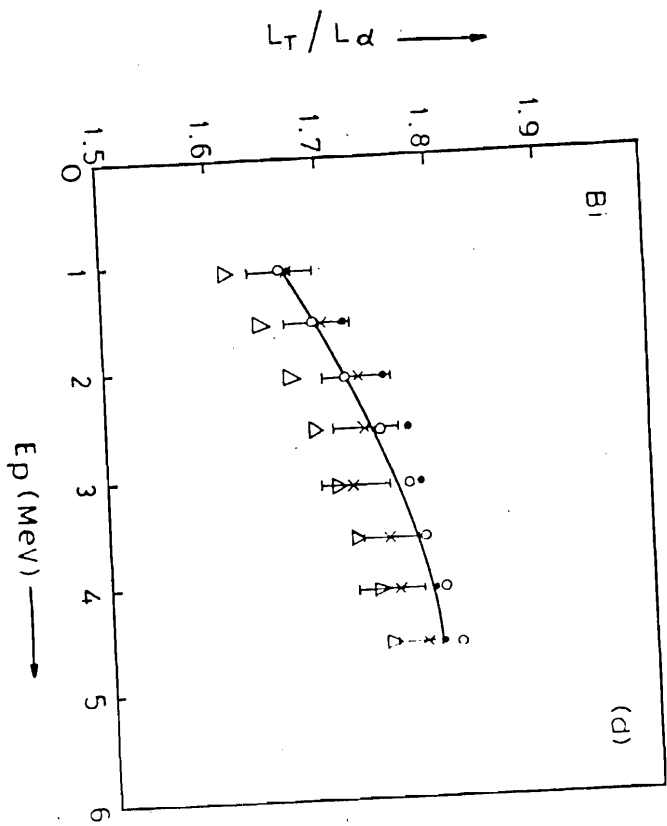


Figure 1

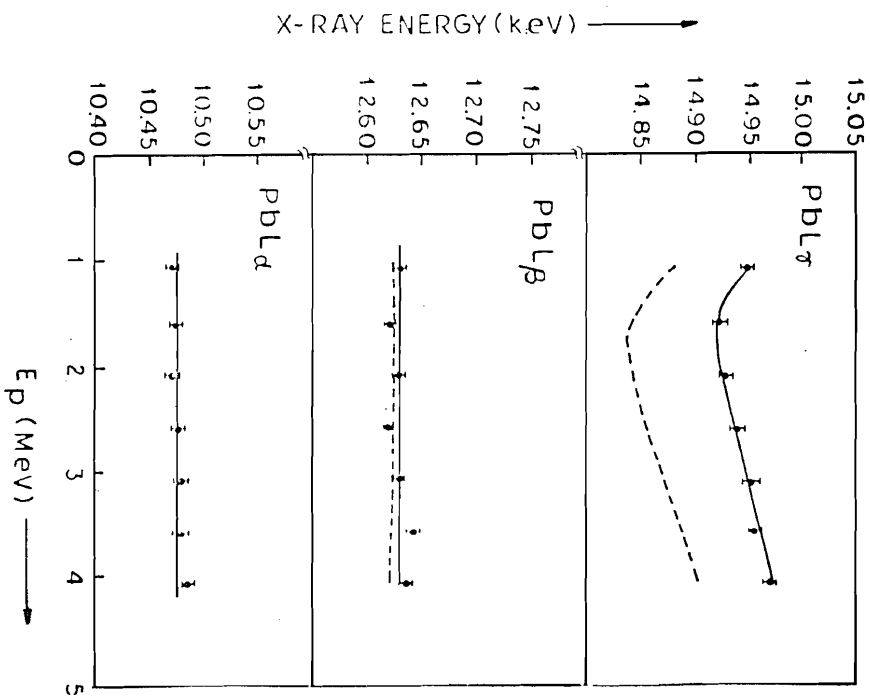
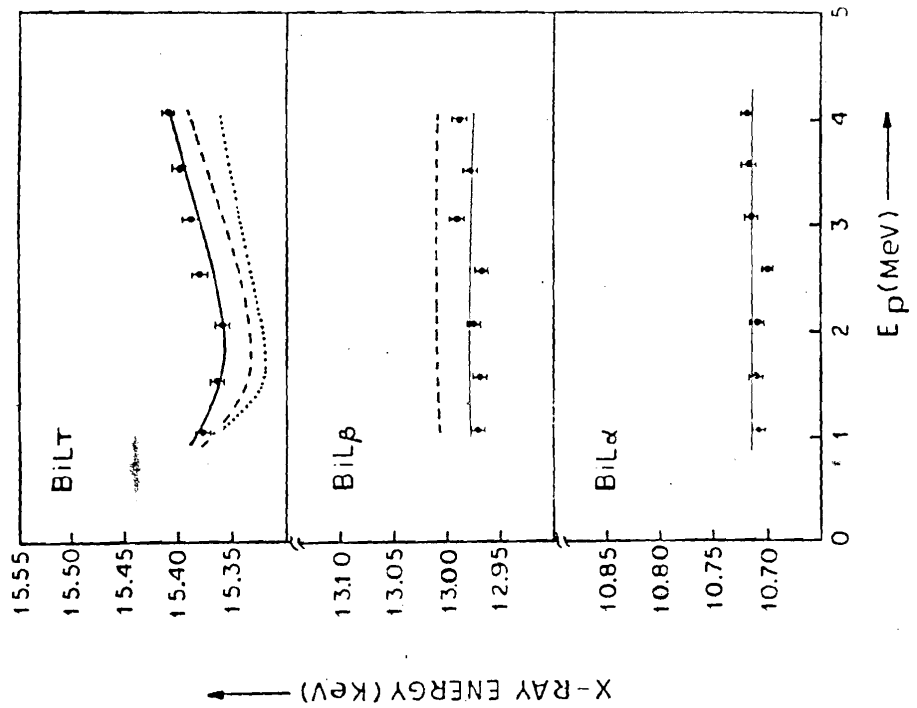


Figure 2



Figure